Influence of oil viscosity on oil-water core-annular flow through a horizontal pipe

van Duin, Erik; Henkes, Ruud; Ooms, Gijs

DOI
10.1016/j.petlm.2018.01.003

Publication date
2018

Document Version
Final published version

Published in
Petroleum

Petroleum 5 (2019) 199–205

Contents lists available at ScienceDirect

Petroleum

journal homepage: www.keaipublishing.com/en/journals/petlm

Influence of oil viscosity on oil-water core-annular flow through a horizontal pipe

Erik van Duin [a], Ruud Henkes [a, b, *], Gijs Ooms [a]

[a] J.M. Burgerscentrum, Delft University of Technology, Faculty of Mechanical, Maritime, and Materials Engineering (3mE), Laboratory for Aero- & Hydrodynamics, Mekelweg 2, 2628 SC Delft, The Netherlands
[b] Shell Projects and Technology, PO Box 38000, 1030 BN Amsterdam, The Netherlands

ARTICLE INFO

Article history:
Received 22 August 2017
Received in revised form
19 December 2017
Accepted 10 January 2018

ABSTRACT

An experimental study has been made of oil-water core-annular flow in a horizontal pipe with special attention for the influence of the oil viscosity on the pressure drop. For that purpose a heating system has been installed and configured that is able to control the oil temperature, such that the oil viscosity could be varied between 3000 cSt at 20 °C and 400 cSt at 50 °C. The oil flow rate was kept at a constant value of 0.35 l/s, whereas the watercut was varied between 9% and 25%. The measured pressure drop is scaled with the calculated pressure drop of only oil flowing at the same flow rate and viscosity.

The main conclusion is that for a large oil viscosity the scaled pressure drop is almost independent of the watercut, whereas with decreasing viscosity the scaled pressure drop becomes strongly dependent on the watercut. Visualisation of the oil-water interface shows a more irregular wave shape with smaller wave lengths when the viscosity is decreased. There is very good agreement between the predictions of the model of Ullmann & Brauner for the scaled pressure drop and the measurements.

1. Introduction

The flow of a core with high-viscosity liquid surrounded by an annulus of low-viscosity liquid is studied through a horizontal pipe. Much attention has been paid in the literature to this type of core-annular flow. Joseph and Renardy [1] have written a book about it. There are several review articles, see for instance Oliemans and Ooms [2] and Joseph et al. [3]. An early publication was by Charles et al. [4]. Studies were published about the stability of core-annular flow and about the transition to other types of flow pattern. Other publications deal with the pressure drop along the pipe and with the hold-up. Many studies deal with the development of waves at the interface between the high and low viscosity liquids. Other review articles on core-annular flow include Ghosh et al. [5] and, as appeared more recently, Shi and Yeung [6].

The present study is focused on the influence of the oil viscosity on core-annular flow. For that purpose we have built an experimental set-up, in which experiments with a very viscous oil and with tap water were carried out in a horizontal pipe. A heating system was installed and configured that is able to control the oil temperature, such that the oil viscosity could be varied. The oil flow rate was kept fixed at a value of 0.35 l/s, whereas the watercut was varied between 9% and 25%. Grassi et al. [7] performed experiments for oil-water flows in a set-up with a similar inner pipe diameter of 21 mm and with comparable oil properties, but they used different types of oil (for a single temperature, namely the room temperature). Based on their produced flow map, we can conclude that our operating conditions are in the stable region of the core-annular flow regime and thus not near a boundary of transition to another flow regime. In the present study a single type of viscous oil is used, for which the viscosity is varied through varying the temperature.

The density of the oil was smaller than the water density, which resulted in an upward buoyancy force on the oil core. This buoyancy force caused the eccentricity of the oil core to be large and hence the water layer at the bottom to be rather thick. Therefore, the flow of water in the annulus at the bottom of the pipe was mostly

* Corresponding author.
E-mail address: R.A.W.M.Henkes@tudelft.nl (R. Henkes).
Peer review under responsibility of Southwest Petroleum University.

Production and Hosting by Elsevier on behalf of KeAi

https://doi.org/10.1016/j.petlm.2018.01.003

turbulent. We checked this by injecting a dye and confirmed that indeed the water flow is turbulent at that location. We have measured the pressure drop as a function of the oil viscosity and as function of the watercut. The wave shape was determined through flow visualisation with a high-speed camera. We also compared the measured pressure drop with model predictions.

2. Experiments

2.1. Experimental setup

Figs. 1 and 2 show schematic overviews of the front side and back side of the experimental set-up. The measurements were carried out in a straight section of the PVC flow loop, which has a diameter of 21 mm. The diameter is constant through the loop. The total length of the flow loop is about 7.5 m and consists of different parts connected to each other with re-attachable links. These pipe sections are in downstream order: a 2 m straight section, a bend with a radius of 0.25 m, a 3 m straight section (the measurement pipe), another bend with a radius of 0.25 m and a straight section of 0.25 m. There is a divider at the inlet to the flow loop, which generates the core-annular flow. The divider has an inner pipe which is concentrically placed within an outer pipe. Oil is entering the flow loop via the inner pipe and water via the annular space between the two pipes. The oil pump and the water flow rate meter were calibrated to enable measuring the oil and water flow rates. Before the inlet device a temperature sensor is placed to measure the oil temperature. After the flow loop the oil-water flow is directed to the separation vessel by a 5 m hose with the same diameter as the PVC pipes. In the separation vessel the oil-water mixture will segregate in approximately 22 h and thereafter the oil can be reused for further experiments. After an experiment the flow loop is rinsed with hot water and a detergent through using a separate rinsing system. Special care is taken for the 3 m measurement pipe which is fully cleaned internally to maintain similar pipe conditions for all experiments. The rising procedure is ended by flushing with warm water only to remove any remaining detergent.

An electronic pressure transducer was connected to two points of the measurement pipe to determine the pressure gradient. The pressure points were at the bottom of the pipe with the rather thick water layer in order to reduce their fouling by the oil as much as possible. The differential pressure transducer has a specified accuracy of 0.5% of the full span, which corresponds to 15 Pa in the present configuration. A small electronic drift in the zero output value is observed and is corrected for by taking a zero measurement prior to each actual measurement. Special attention is paid to the alignment of the pressure tubes to be flushed with the pipe wall; a small offset, however, cannot completely be excluded. This reduces the accuracy of the pressure drop measurement slightly. The volumetric water flow rate is measured with a digital flow meter, which gives 1150 pulses per litre. Multiple calibration measurements result in an accuracy of this device that is within 4% of the actual flowrate. The flow rate produced by the oil pump is set by a variable frequency drive which is recorded during the measurements. The calibration of the oil pump resulted in a volumetric oil flow rate within 1% accuracy. The temperature of the oil entering the flow loop increases by 0.5 °C during a typical experiment, which is caused by the oil pump. The increase in temperature results in a decrease in oil viscosity. Especially at low temperatures, the dependency of the oil viscosity is stronger and therefore results in larger deviations in the actual condition. The sensors are connected to a data acquisition board which is linked to a computer in order to monitor and save the data. The differential pressure transducer, oil flow rate and oil temperature are sampled at 100 Hz, whereas the water flow rate is recorded at 1 Hz. The typical experimental time of the settled core-annular flow is around 65 s. The experiments were repeated several times to check their reproducibility.

The (Newtonian) oil used for the experiments is Shell Morlina S2 B 680. As mentioned, a heating system was installed to control the oil temperature. The dependency of the oil viscosity on the temperature is determined by a rheometer of *TA Instruments*, type *AR-G2*. The variation in oil kinematic viscosity used in the experiments is from 3000 cSt (or 0.003 m^2/s) at 20 °C to 400 cSt (or 0.0004 m^2/s) at 50 °C. The oil density ρ_{oil}, as measured with an Anton Paar density meter, slightly decreases from 913 kg/m^3 at 20 °C to 895 kg/m^3 at 50°. The interfacial tension was measured with a Krüss ring

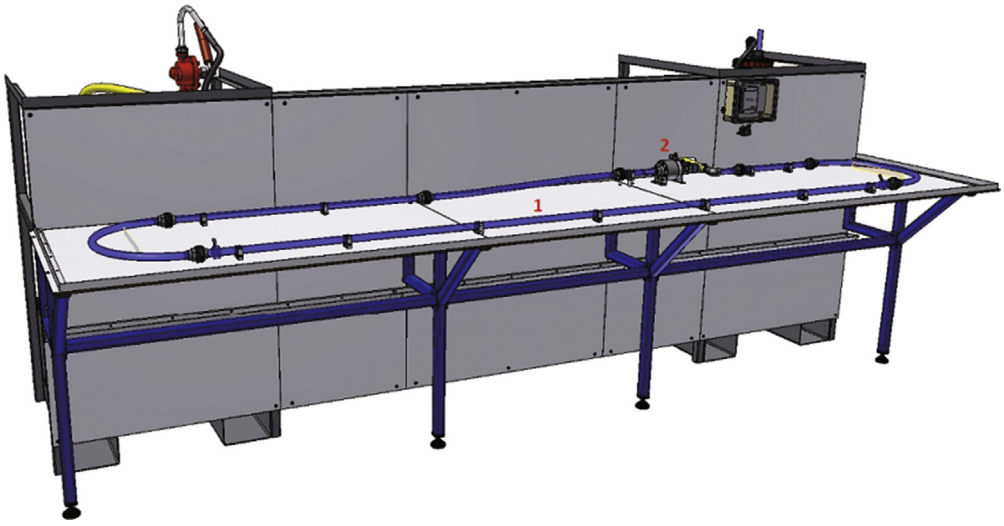

Fig. 1. Schematic overview of the front side of the experimental set-up.
Item 1: Measurement pipe of the flow loop. Item 2: Divider.

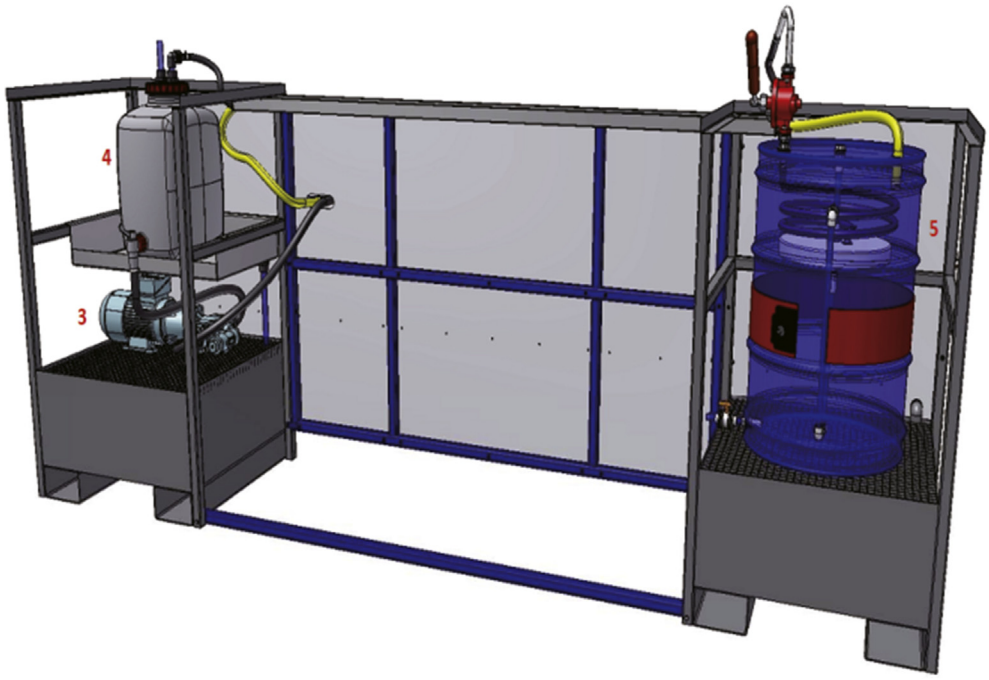

Fig. 2. Schematic overview of the back side of the experimental set-up.
Item 3: Oil pump. Item 4: Oil container with a copper coil inside to heat up the oil. Item 5: Separation vessel for oil and water.

tensiometer, and its value is equal to $\sigma = 0.014$ N/m at 20 °C; the corresponding value of the Eötvös number, defined as $Eo = (\rho_{water}-\rho_{oil})gD^2/\sigma$, is equal to 27 (note that g is the gravitational acceleration and D is the pipe diameter).

The oil flow rate was kept at a value of 0.35 l/s (which corresponds to a superficial oil velocity of 1.01 m/s), whereas the watercut is varied as 9%, 12%, 15%, 20% and 25% (corresponding to superficial water velocities between 0.1 m/s and 0.34 m/s). Note that the watercut is defined as follows:

$$watercut \equiv \frac{Q_{water}}{Q_{oil} + Q_{water}}, \quad (1)$$

where Q_{oil} and Q_{water} are the oil and water volumetric flowrates, respectively.

Flow visualisation was realized with a *Vision Research*high-speed camera at a rate of 1000 fps with an exposure time of 80 μs? The camera has a 5 megapixel, 12-bit grey scale CMOS optical chip. A LED light panel is placed under the imaging box and an additional light source is placed near the imaging region to obtain sufficiently illuminated images. A transparent box filled with water was placed around the measurement pipe to improve the quality of the recordings. This removed the distortions from the pipe wall and it also helped to focus the camera at the top and bottom parts of the pipe, where the most interesting flow aspects of core-annular flow occur. To capture the behaviour of the core in the horizontal plane, i.e. at the front and back of the interface, a mirror was placed on top of the imaging box. This enabled us to record a top and front view of the core-annular flow interface simultaneously. A photograph of this part of the setup is presented in Fig. 3. The change in optical path lengths between the top and front view is corrected by placing a box of water in the path of the top view. This was necessary to reduce the focal depth of the camera.

2.2. Experimental results for the pressure drop

Ingen Housz et al. [8] carried out experiments in almost the same experimental set-up. In our set-up an electronic pressure transducer was used instead of an inverted U-tube manometer applied by Ingen Housz et al. They used Morlina S4 B 680 as viscous liquid with a density of 860 kg/m^3 at room temperature. The oil in our experiments has a slightly larger density of 913 kg/m^3 (at 20 °C). For both oils, the viscosity as function of the temperature is nearly identical. It is thus interesting to compare our results with those of Ingen Housz et al. Their experiments were performed at

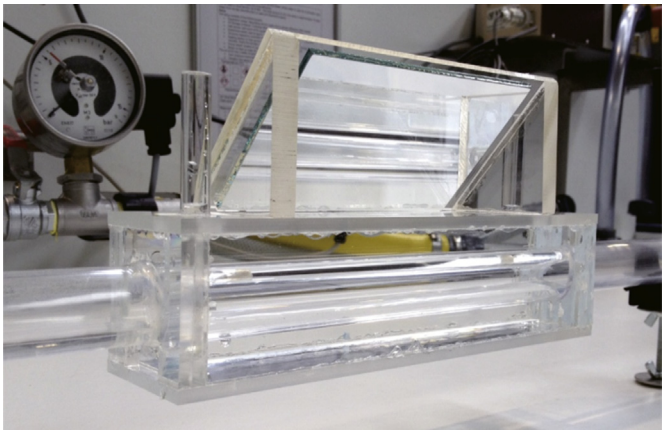

Fig. 3. Photograph of the box used for flow visualisation. A mirror is placed on top of the box in order to capture the front/back of the water annulus simultaneously with the top/bottom water layer.

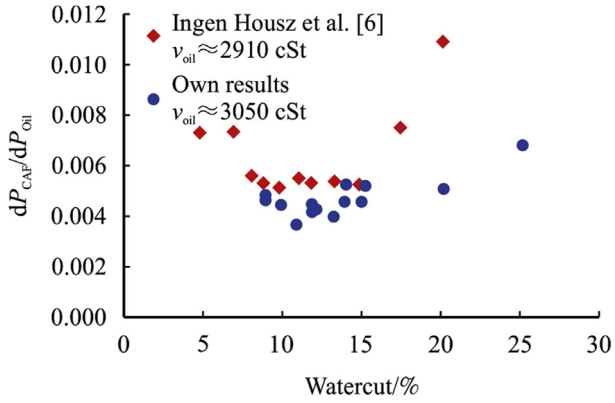

Fig. 4. Comparison of the current measurements for scaled pressure drop with those of Ingen Housz et al. [6].

certain selected values of the oil flow rate, Q_{oil}, during which the water flow rate was decreased (starting from a relatively large watercut). Only experiments at room temperature were performed. Our experiments were done in a similar way; however, now only one oil flow rate is set, namely Q_{oil} is 0.35 l/s, for which the oil temperature and watercut were varied. Our results at room temperature can directly be compared with the results of Ingen Housz et al.: Fig. 4 shows both results for the scaled pressure drop as function of the watercut. Note that the measured pressure drop for core-annular flow is scaled by using the calculated pressure drop when oil alone is flowing with the same flow rate and viscosity, see equation (2).

Overall a similar trend is observed between the two sets of experiments, where a minimum in the scaled pressure drop is found at a watercut between 10% and 14%. In general, our measured scaled pressure drops are lower than those measured by Ingen Housz et al. A first explanation for the difference is the oil viscosity at room temperature. Comparison of the kinematic viscosity of the oil (3050 cSt in our experiments versus 2910 cSt in the experiments by Ingen Housz et al.) shows a slightly lower value as used by Ingen Housz et al. As will be discussed later, decreasing the oil viscosity will increase the scaled pressure drop dP_{CAF}/dP_{oil}. Since the oil viscosity in our experiments is slightly larger, the value of the scaled pressure drop is smaller. A second reason for the difference in the scaled pressure drop is the density difference between oil and water. Since our oil is denser, our density difference between oil and water is smaller. Therefore, the upward buoyancy force on the core is lower, which leads to a less eccentric oil core. The water annulus at the bottom becomes thicker when the core is more eccentric. The pressure points are located at the bottom of the pipe and the measurement could be influenced by the thicker water layer. Especially for a larger watercut (>18%) this effect becomes more dominant, which might contribute to the deviation between the two experimental data sets.

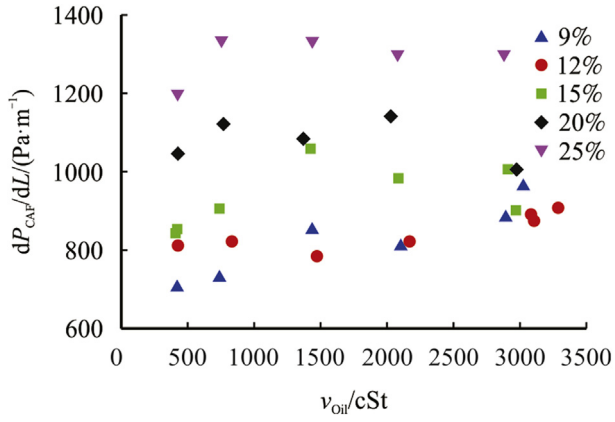

Fig. 5. Measured (non-scaled) pressure drop for core-annular flow as function of the oil viscosity at different values of the watercut.

Fig. 5 presents all values of the measured (non-scaled) pressure gradient, dP/dL, as a function of the oil kinematic viscosity, ν_{oil}, for different values of the watercut. The oil viscosity decreases with increasing temperature; the viscosity varies between about 3000 cSt at 20 °C and about 400 cSt at 50 °C.

At the considered watercuts, there seems to be a trend that the pressure gradient decreases with decreasing oil viscosity. At largest considered watercut of 25% the pressure gradient is almost independent of the oil viscosity.

For all oil viscosities, an increasing watercut gives an increase of the scaled pressure gradient. This is due to the increase in the water flow rate at constant oil flow rate, which results in a larger total flow rate.

Fig. 6 gives an overview of all values of the measured scaled pressure drop, dP_{CAF}/dP_{oil}, as a function of the viscosity ratio of the high and low viscous fluids, ν_{oil}/ν_{water}, at all watercuts. With increasing temperature, the viscosity ratio decreases. It ranges again between ν_{oil}/ν_{water} ~400 at 50 °C and ν_{oil}/ν_{water} ~3000 at 20 °C. It is important to point out that the measured pressure gradient has been scaled with the calculated value of only the laminar flow of oil through the pipe at the same viscosity values as, which reads:

$$\frac{dP_{oil}}{dL} = \frac{128}{\pi}\frac{\nu_{oil}\rho_{oil}Q_{oil}}{D^4}, \tag{2}$$

where ν_{oil} is the oil kinematic viscosity and ρ_{oil} is the oil density (both at the measured temperature), Q_{oil} is the measured oil flow rate and D is the pipe diameter. It could thus be expected that dP_{CAF}/dP_{oil} increases with temperature.

Fig. 6 shows that dP_{CAF}/dP_{oil} decreases with increasing oil viscosity. This means that the relative advantage of adding water to form a lubrication layer along the pipe wall is larger in case the oil is more viscous. The figure also shows that for the highest considered oil viscosity, i.e. the one at room temperature, the value of dP_{CAF}/dP_{oil} is almost independent of the watercut. But for a decreasing viscosity, the scaled pressure drop increases with the watercut. This is because the benefit of water lubrication at low oil viscosity is less, and here the fact that water is added in a larger amount at higher watercut increases the total throughput which reduces the benefit of using water as lubrication even more.

2.3. Flow visualisation results

Figs. 7 and 8 display recorded pictures for the typical flow patterns of core-annular flow at watercuts of 12% and 20%, respectively. The flow direction is from the left to the right. The “top view” images in the figures show the water annulus on the left and right side of the oil core in the horizontal pipe, whereas the “front view” images show the water annulus below and above the oil core. For the left images, the oil temperature is 23 °C, corresponding to an oil viscosity of approximately 2500 cSt, whereas for the right images the oil temperature is close to 40 °C, corresponding to an oil viscosity of approximately 780 cSt. All images are post-processed to enhance the contrast of the oil-water interface. The streamwise length of the images is approximately 4 inner pipe diameters, which proved to be sufficient to capture the structures present on the oil-water interface. The top view image displays the flow as

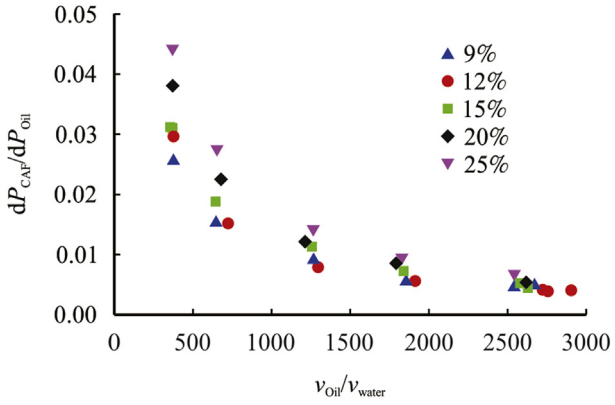

Fig. 6. Scaled pressure drop as function of the viscosity ratio at different values of the watercut.

seen through the mirror, where the interface at the top in this image is closest to the camera. The bright parts seen on the core are reflections of the light source.

Comparing the top and front view shows that the oil core is eccentrically positioned in the front view due to the upward buoyancy force, whereas the top view displays the core concentrically located in the pipe. However, the oil core appears also to be eccentrically located in the top view images, which is in contradiction to visual observation during the experiments. This can be the result of imperfections in the visualisation box in combination with artefacts due to the pipe curvature. As expected, the water annulus becomes thinner when the watercut is decreased, making it harder to observe the interface at the top of the pipe. At some locations it seems that the oil core touches the pipe wall. Since no fouling is observed during the experiments, it can be concluded that the core is properly lubricated.

In all images waves are present on the oil-water interface. The front view shows that the wave crest, i.e. the interface closest to the wall, has a phase delay; the wave crest at the bottom is ahead of the wave crest present at the top of the core. In the top view, however, the wave crests are at almost the same streamwise location. This behaviour is more clearly observed for large watercuts (Fig. 7), but is also present at low watercuts.

For low oil viscosity, oil drops are present around the core; see for example the light grey circular objects in the middle of the core of the front view of Fig. 7 on the right. It is observed that these drops are formed at the divider where the oil core is injected. The oil drops are in the water annulus, but are still fully surrounded by water since the pipe wall is not fouled after a drop has passed.

When comparing the images for high and low oil viscosity, it is observed that the core is less smooth for low oil viscosity. The wave lengths present on the interface become shorter when the oil viscosity is decreased. Furthermore, a clear wave length is not observed anymore. Since the oil viscosity is decreased, the core is more easily deformed by the hydrodynamic forces of the water annulus that keep the core lubricated.

A future prospect of the visualisation study will be to obtain quantitative information of the core-annular interface, such as the core eccentricity, and the amplitude and length of the wave present on the oil-water interface. These experimental data can for example be used for the comparison with ongoing detailed numerical simulations.

3. Model predictions versus experiments

The measurements for the pressure drop were compared with the predictions from the model as proposed by Ullman and Brauner [9]. This is a mechanistic, two-fluid model that assumes a concentric laminar oil core, and a turbulent water annulus. The oil and water velocity profiles are approximated by a single bulk oil velocity and a single bulk water velocity, respectively, with slip between the phases. The model is closed by using a friction law for the shear stress between the water film and the wall, and a friction law for the interfacial stress between the oil core and the water annulus. For the applied friction laws, a closed form of the solution of the model can be obtained.

The model solution for the scaled pressure drop is:

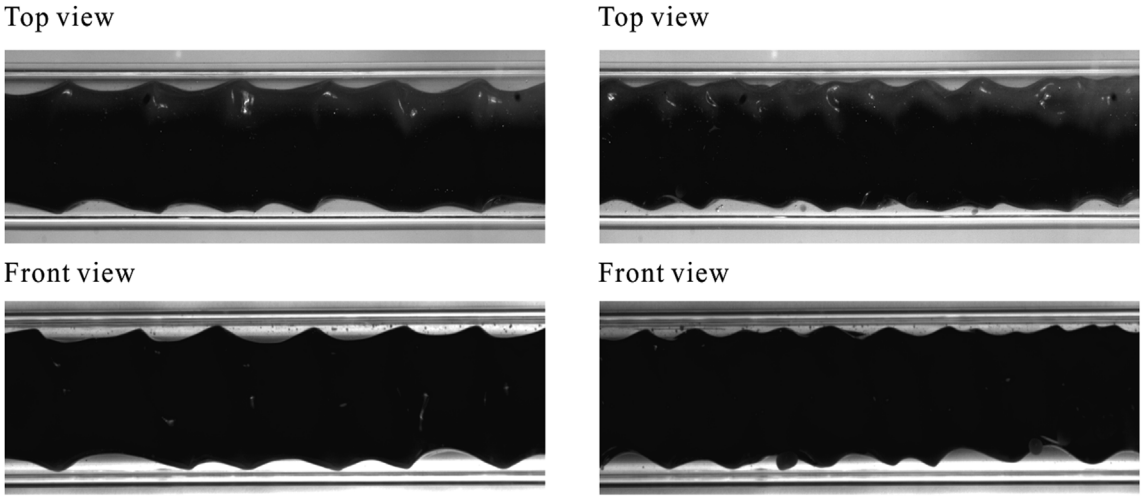

Fig. 7. Flow visualisation of core-annular flow for an oil flow rate of 0.35 l/s and a watercut of 20%. Left: oil viscosity of 2500 cSt ($T_{oil} \approx 23.4\,^{\circ}C$). Right: Oil viscosity of 768 cSt ($T_{oil} \approx 39.0\,^{\circ}C$).

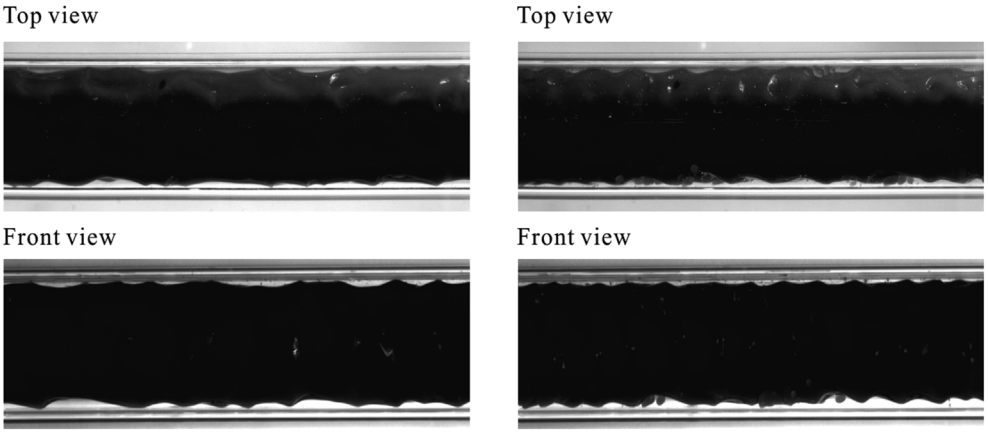

Fig. 8. Flow visualisation of core-annular flow for an oil flow rate of 0.35 l/s and a watercut of 12%. Left: oil viscosity of 2480 cSt ($T_{oil} \approx 23.5\,^{\circ}C$). Right: Oil viscosity of 784 cSt ($T_{oil} \approx 38.7\,^{\circ}C$).

$$\frac{dP_{CAF}}{dP_{oil}} = \frac{X^2}{\alpha_{water}^2}, \tag{3}$$

in which $X^2$is the Lockhart-Martinelli parameter (being the ratio of the pressure drop found for single phase water flow and the pressure drop found for single phase oil flow) and α_{water} is the water holdup fraction (being the fraction of the pipe cross sectional area covered by the water annulus). The model has the following solutions for the Lockhart-Martinelli parameter and for the water holdup fraction:

$$X^2 = \frac{0.046}{16}\left(\frac{\nu_{water}}{\nu_{oil}}\right)^{0.2}\frac{\rho_{water}}{\rho_{oil}}\frac{\mathrm{Re}_{s,oil}^{0.8}}{Q^{*1.8}}. \tag{4}$$

$$\alpha_{water} = \frac{0.5\ c_i - X^2Q^*/F_i + 0.5\ c_i\sqrt{1+4X^2(Q^*/c_i)^2/F_i}}{c_i + Q^* - X^2Q^*/F_i}. \tag{5}$$

where $\mathrm{Re}_{s,oil} = \frac{U_{s,oil}D}{\nu_{oil}}$ and $Q^* = \frac{Q_{oil}}{Q_{water}}$; the superficial oil velocity is defined as $U_{s,oil} = \frac{Q_{oil}}{\pi D^2/4}$, in which D is the pipe diameter. The coefficients c_i and F_i are model constants in the relation for the interfacial stress, which are taken as, following Ullman and Brauner [9], $c_i = 1.17$ and $F_i = 1$.

The comparison between the predicted and measured values for the scaled pressure drop is shown in Fig. 9. All measured values for the considered watercuts and oil viscosities are included. There is a very good agreement between the model predictions and the measurements, as all values fall within the 20% accuracy interval.

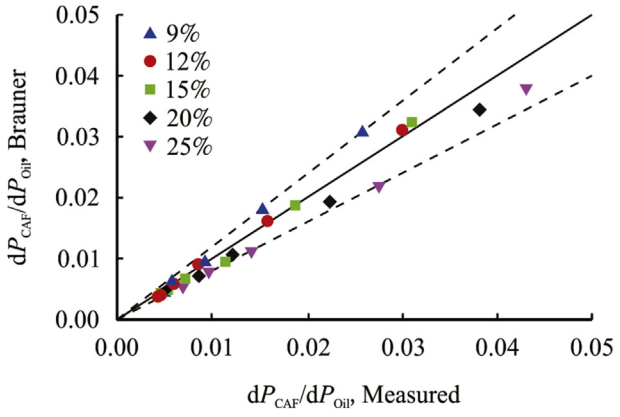

Fig. 9. Predicted scaled pressure drop versus the measured value. The solid line denotes perfect agreement, and the dashed lines denote the 20% accuracy interval.

4. Conclusions

Pressure drop measurements for oil-water core-annular flow were performed and compared to previous results by Ingen Housz et al. In the present study, the oil viscosity is decreased by increasing the oil temperature to investigate the influence of the oil viscosity on the pressure drop at different watercuts. The scaled pressure drop as function of the viscosity ratio is presented, from which it is concluded that transport by means of core-annular flow is more beneficial at a high viscosity ratio (note that the measured pressure drop is scaled with the pressure drop in the presence of oil only, at the same flow rate and viscosity). At a lower viscosity ratio the amount of water needed to lubricate the oil core causes an increase in the scaled pressure drop and thus the effect of the total throughput becomes more present. The mechanistic model of Ullman & Brauner gives a very good reproduction of the measured scaled pressure drop, as all predictions fall within the 20% accuracy interval.

The flow visualisation study shows a clear distinction in the oil-water interface when decreasing the oil viscosity. The waves present on the interface become shorter in length and more irregular when the oil viscosity is decreased. This is present for both large and small watercuts. Furthermore, for decreasing oil viscosity, oil drops are observed in the water annulus. Since the pipe wall is clean after an experiment it can be concluded that oil is still properly lubricated by water in all experiments.

References

[1] D.D. Joseph, Y.Y. Renardy, Fundamentals of Two-fluid Dynamics, Part II: Lubricated Transport, Drops and Miscible Liquids, Springer-Verlag, New York, 1993.
[2] R.V.A. Oliemans, G. Ooms, Core-annular flow of oil and water through a pipeline, Multiphas. Sci. Technol. 2 (1986) 427–476.
[3] D.D. Joseph, D. Bai, K.P. Chen, Y.Y. Renardy, Core-annular flows, Annu. Rev. Fluid Mech. 29 (1999) 65–90.
[4] M.E. Charles, G.W. Govier, G.W. Hodgson, The horizontal pipeline flow of equal density oil-water mixture, Can. J. Chem. Eng. 39 (1961) 27–36.
[5] S. Ghosh, T.K. Mandal, G. Das, P.K. Das, Review of oil water core annular flow, Renew. Sustain. Energy Rev. 13 (2009) 1957–1968.

[6] J. Shi, H. Yeung, Characterization of liquid-liquid flows in horizontal pipes, AIChE J. 63 (2017) 1132–1143.
[7] B. Grassi, D. Strazza, P. Poesio, Experimental validation of theoretical models in two-phase high-viscosity ratio liquid-liquid flows in horizontal and slightly inclined pipes, Int. J. Multiphas. Flow 34 (2008) 950–965.
[8] E.M.R.M. Ingen Housz, G. Ooms, R.A.W.M. Henkes, M.J.B.M. Pourquie, A. Kidess, R. Radhakrisnan, A comparison between numerical predictions and experimental results for core-annular flow with a turbulent annulus, Int. J. Multiphas. Flow 95 (2017) 271–282.
[9] A. Ullmann, N. Brauner, Closure relations for the shear stress in two-fluid models for core annular flow, Multiphas. Sci. Technol. 16 (2004) 355–387.